Flight-Test System Identification Methodology and Hover Results for a Vectored-Thrust eVTOL Aircraft

Benjamin M. Simmons

Research Aerospace Engineer Flight Dynamics Branch NASA Langley Research Center Hampton, VA, USA

Andrew Rapsomanikis

Technical Lead – Flight Control Software

NK Ofodile

Head of Systems Engineering

George Jacobellis

Head of Flight Sciences

Thomas Hamilton

Staff GN&C Engineer

Max Ma
President, Partner
AIBOT
Torrance, CA, USA

ABSTRACT

This paper describes an ongoing aircraft system identification effort for an industry prototype electric vertical takeoff and landing (eVTOL) vehicle. Building on previous eVTOL aircraft system identification developments in wind-tunnel testing and flight simulations, an approach to modeling from flight-test data is formulated for the AIBOT 500 aircraft. The full system identification process is presented, including the experiment design, flight data collection, and model identification steps. Orthogonal phase-optimized multisine programmed test inputs are integrated into the flight control system and are applied to each control surface and propulsor simultaneously to efficiently collect informative flight data for model identification. Initial modeling results are given in hover, where an aero-propulsive model is identified using the equation-error method in the frequency domain. The presented results demonstrate the utility of the modeling approach and are compared to FLIGHTLAB® predictions executed using a dynamic wake model made prior to conducting flight testing. Practical techniques and recommended improvements are discussed to inform future flight-test system identification efforts for eVTOL aircraft.

NOTATION

a_x, a_y, a_z	body-axis translational acceleration, ft/s ²
I_x, I_y, I_z	aircraft moments of inertia, slug·ft ²
L, M, N	body-axis aero-propulsive moments, ft·lb:
m	aircraft mass, slug
$\Omega_1,\Omega_2,,\Omega_8$	proprotor rotational speeds, rad/s
p, q, r	body-axis angular velocity components,
	rad/s
u, v, w	body-axis translational velocity
	components, ft/s
X, Y, Z	body-axis aero-propulsive forces, lbf
$\delta_1, \delta_2,, \delta_8$	control surface deflection angles, rad
$\phi, heta, \psi$	Euler roll, pitch, and yaw angles, rad

Presented at the Vertical Flight Society's 81st Annual Forum & Technology Display, Virginia Beach, VA, USA, May 20–22, 2025. This material is declared a work of the U.S. Government and is not subject to copyright protection in the United States.

INTRODUCTION

Development of practical vehicles for Advanced Air Mobility (AAM) applications has recently been enabled by hybrid and electric distributed propulsion aircraft technology advancements. A critical part of AAM is Urban Air Mobility (UAM), which requires vehicles that can takeoff and land vertically, precisely maneuver at low speeds, and safely transition to more efficient high-speed cruise flight. Electric vertical takeoff and landing (eVTOL) vehicles have emerged as a promising candidate to support UAM operations. Many eVTOL aircraft designs are currently being investigated, including tiltwing, tiltrotor, and lift+cruise configurations (Refs. 1–9). The vehicles generally include features from traditional fixed-wing and rotary-wing aircraft, as well as new distributed electric propulsion attributes that have substantially broadened the traditional aeronautical vehicle design space.

Although eVTOL aircraft have great potential to revolutionize the aviation industry, there are several areas of study to be addressed before the vehicles can be used for sustained operation in an urban air traffic system. Current research areas include airworthiness certification, handling qualities, flight controls, air traffic management, contingency management, and autonomy, among others. Research in each of these areas benefits from being able to accurately predict eVTOL aircraft flight motion, thereby making flight dynamics simulations driven by accurate aero-propulsive models a critical enabling capability. Efficient and accurate eVTOL aircraft aero-propulsive model development for use in flight dynamics simulations, however, is challenged by complex eVTOL vehicle attributes such as many control surfaces and propulsors, propulsion-airframe aerodynamic interactions, unstable vehicle dynamics, rapidly changing aerodynamics through transition, and a wide range of operational flight conditions to characterize.

The goal of a flight vehicle aero-propulsive model is to accurately describe the aerodynamics in flight, which drive aircraft flight dynamic behavior. Accordingly, aerodynamic characterization using flight data usually offers the closest prediction to operational reality. This work builds on previous eV-TOL aircraft modeling studies to formulate and demonstrate a method for flight-based aero-propulsive model development.

The process of developing mathematical models describing aircraft dynamics from measured input and output data is referred to as aircraft system identification (Refs. 10-12). The aircraft system identification process generally involves identifying a mathematical representation of the applied forces and moments as a function of state and control variables, based on experimental data. System identification techniques are well developed for many fixed-wing and rotary-wing aircraft modeling problems (Refs. 13-18); however, the unexplored aspects of eVTOL aircraft system identification and overcoming complex eVTOL aircraft configuration challenges to efficiently produce an accurate aero-propulsive model require further study. Presentation of a method for eVTOL aircraft system identification using flight-test data from an industry prototype eVTOL vehicle will be the primary subject of this paper.

The remainder of the paper is organized as follows. First, related aircraft system identification research is summarized. Subsequent sections introduce the experimental aircraft and outline previous aerodynamic characterization efforts. Next, the flight-test system identification approach is described, followed by an overview of the system-identification-related flight-test risk-reduction steps. The paper closes with presentation of preliminary hover modeling results and concluding remarks.

BACKGROUND

Recent aircraft system identification research with similar challenges to eVTOL vehicles is briefly highlighted to provide context for the present work. Reference 19 presented an

approach for efficient estimation of the effectiveness of 16 different control surfaces on a generic commercial transport aircraft using the frequency-domain equation-error method. Orthogonal phase-optimized multisine signals were injected into each control surface allowing individual control derivatives to be identified simultaneously from the data collected during a single flight maneuver. System identification of the X-56 aeroelastic technology demonstrator aircraft employed a similar approach (Refs. 20–22). A collection of different multisine signals was designed to excite the control effectors—10 control surfaces and two engines—independently and in pairs for efficient model identification using frequency-domain modeling methods (Ref. 23). Reference 24 describes system identification for a fixed-wing aircraft with eight distributed electric ducted fans (EDFs). Multisine signals were applied to control surfaces and throttle doublets were applied to individual EDFs to identify linear longitudinal and lateral-directional state-space models.

Numerous contemporary studies have identified models for multirotor vehicles from flight data with various input type using both frequency-domain and time-domain system identification techniques (Refs. 25–36). Reference 37 describes system identification for a quadrotor configuration intended for a UAM mission demonstrated using simulated flight data. Frequency sweeps were applied to each pilot control input to generate data for frequency response and state-space model identification. References 38 and 39 applied multisine signals to each propulsor on multirotor vehicles to estimate linear dynamic models. Recent system identification efforts have been pursued for lift+cruise eVTOL aircraft configurations using time-domain (Ref. 40) and frequency-domain (Ref. 41) system identification approaches.

This paper primarily builds on publications that documented wind-tunnel testing, aero-propulsive modeling, and system identification research conducted using the NASA LA-8 and RAVEN-SWFT aircraft (Refs. 42–47). The LA-8 is a subscale tandem tiltwing eVTOL aircraft and the RAVEN-SWFT is a subscale tiltrotor eVTOL aircraft, both built by NASA Langley Research Center as testbeds for eVTOL aircraft technology (Refs. 8, 9, 48).

Reference 42 describes the aero-propulsive model development process applied for the LA-8 aircraft. Static poweredairframe wind-tunnel testing was conducted using design of experiments (DOE) and response surface methodology (RSM) test techniques (Refs. 49, 50) to collect data for creating an aero-propulsive model of the aircraft through its transition envelope. Because eVTOL vehicle configurations exhibit aerodynamic characteristics of both fixed-wing and rotarywing aircraft, as well as complex vehicle-specific phenomena, traditional aircraft aerodynamic modeling strategies require modification when applied to eVTOL aircraft. Hence, in Ref. 42, significant focus was placed on development and justification of empirical aero-propulsive modeling strategies for eVTOL aircraft using wind-tunnel data; this included postulating the definitions of modeling explanatory variables and response variables, designing experiments to enable efficient and accurate characterization of pertinent aerodynamic phenomena, development of approaches to accurately model the aircraft over the full transition flight envelope, and investigation of the aero-propulsive coupling that is ubiquitous for eV-TOL vehicles. The final LA-8 aero-propulsive model consisted of a set of nonlinear response surface equations describing the aero-propulsive forces and moments exerted on the aircraft at several discrete reference airspeed conditions throughout the vehicle flight envelope. Reference 43 applied a similar approach to the RAVEN-SWFT aircraft with numerous wind-tunnel testing and experiment design improvements. Building on this static wind-tunnel testing research, Ref. 44 developed a new modeling approach for the LA-8 eVTOL aircraft leveraging a more efficient wind-tunnel experiment that used a combination of DOE/RSM techniques and orthogonal phase-optimized multisine signals applied to control surfaces and propulsors. Significant emphasis was placed on multisine signal design for eVTOL aircraft and formulation of a multistep frequency-domain modeling process.

Based on the findings gleaned from LA-8 wind-tunnel experiments, Ref. 45 presented a flight-test system identification strategy for transitioning eVTOL aircraft demonstrated using a high-fidelity flight dynamics simulation. Orthogonal phase-optimized multisine inputs were applied to each control surface and propulsor at numerous trimmed flight conditions throughout the flight envelope to collect informative simulated flight data enabling aero-propulsive model identification at each condition. The identified models were shown to provide a good fit to modeling data and have similar prediction capability for validation data. The methodology was developed with a discussion of unique eVTOL vehicle aerodynamic characteristics and practical strategies intended to inform future flight-based system identification efforts for eV-TOL aircraft. Although this LA-8 flight simulation study was informative, a clear next step is verification of the techniques using actual flight-test data for an eVTOL aircraft. A related effort for the RAVEN-SWFT applied a similar method to free motion wind-tunnel testing for aero-propulsive damping characterization, providing initial experimental validation of the approach in the rotational degrees of freedom (Ref. 46). Furthermore, initial flight testing for the RAVEN-SWFT has begun to demonstrate a similar flight-test system identification approach (Ref. 47).

This current paper expands on previous work to describe and demonstrate an efficient eVTOL aircraft system identification approach that uses flight-test data from an industry prototype eVTOL aircraft, described next. Practical flight-test strategies, the current modeling approach, and findings from initial hover testing for this ongoing effort are the focus and new contributions of this paper.

AIRCRAFT

The eVTOL vehicle used in this work is the AIBOT 500 aircraft designed, built, and flight tested by AIBOT. The AIBOT 500 is a prototype 500-lb vectored-thrust eVTOL aircraft configuration that is equipped with eight control surfaces

and eight proprotors. The control surface deflection angles are denoted $\delta_1, \delta_2, ..., \delta_8$ and the propulsor rotational speeds are denoted $\Omega_1, \Omega_2, ..., \Omega_8$. Each of the control surfaces is located within the wake from the proprotors in all phases of flight. The AIBOT 500 aircraft configuration is currently not in the public domain, therefore, the paper will discuss the vehicle in the generic context of a transitioning vectored-thrust eV-TOL aircraft configuration. The AIBOT 500 aircraft details are expected to be publicly revealed in the future—public information can be found on AIBOT's website (Ref. 51).

The mass and horizontal center of gravity of the AIBOT 500 vehicle were determined empirically. The vehicle moments of inertia were estimated using a component build-up approach. The roll and pitch moment of inertia estimates (I_x and I_y , respectively) were validated using the flight-derived hover rolling and pitching moment propulsor control derivatives presented later in the paper. These flight-test system identification results, along with thrust stand data, known aircraft geometry, and an assumption that the hover propulsion-airframe interaction effects are negligible in the rolling and pitching moment responses, provided an alternative way to solve for I_x and I_y . The agreement of the I_x and I_y estimates computed in different ways bolstered confidence that the mass properties build-up approach yielded accurate vehicle moments of inertia.

A commercial flight computer is used to operate the AIBOT 500 aircraft with a custom AIBOT flight control algorithm, which was augmented with an automated programmed test input (PTI) injection capability for system identification. The flight computer interfaces with and enables high-rate logging of aircraft instrumentation used for system identification, which included an inertial measurement unit (IMU), inertial navigation system (INS), and electronic speed controller (ESC) feedback. The IMU provides accelerometer and angular rate gyroscope measurements; the INS provides vehicle attitude and inertial body-axis velocity state estimates; the ESCs provide commanded and actual motor rotational speed, among other signals. Additional logged data include the control surface servo-actuator commands and ESC commands from the flight computer, as well as the PTI signals for one motor and servo, which indicate where PTIs are enabled and their amplitude. All data used for system identification are logged at a 50 Hz sample rate, except for the ESC data, which are logged at 10 Hz.

BASELINE AERODYNAMIC PREDICTIONS

Prior to conducting flight testing, multiple efforts were pursued to characterize the AIBOT 500 aircraft aerodynamics. Thrust stand testing was performed with a single proprotor to determine isolated performance characteristics and verify the reliability of electronic components used to conduct flight

The use of trademarks or names of manufacturers in this report is for accurate reporting and does not constitute an official endorsement, either expressed or implied, of such products or manufacturers by the National Aeronautics and Space Administration.

testing. Additionally, FLIGHTLAB® (Ref. 52) was used to predict the performance of the isolated proprotor, as well as the full integrated vehicle. Aerodynamic predictions from FLIGHTLAB® using a dynamic wake model for the proprotors will be compared to flight-test derived results later in the paper.

SYSTEM IDENTIFICATION APPROACH

The process for aircraft system identification from flight data generally follows the steps outlined in Figure 1. System identification efforts are often motivated by an application that requires an accurate dynamic model, such as control law design/tuning or validation of aerodynamic predictions obtained from analytical techniques, computational fluid dynamics, and/or ground testing. The desired model accuracy and range of applicability for the intended application set objectives for the aircraft system identification effort. Next, a flight-test experiment is designed and conducted to excite the aircraft dynamics over the regions of desired model applicability. After collecting the flight data, a series of data processing steps are used to assess the data quality and condition the measured flight data for model identification. The model structure is then determined from the measured data and model parameters within the model structure are estimated. The identified model is subsequently validated to assess its accuracy and prediction capability, as well as the adequacy of the model for its intended application. If the model is inadequate, then remedial plans are developed for additional testing that can provide the data required to identify an adequate model. If the model is deemed sufficient, then it may be used for an intended application. The remainder of this section will provide additional details on each part of the system identification process, as applied for the AIBOT 500 aircraft. The input design and parameter estimation methods used for this work were adapted from the System IDentification Programs for AirCraft (SID-PAC) software toolbox (Refs. 10, 53).

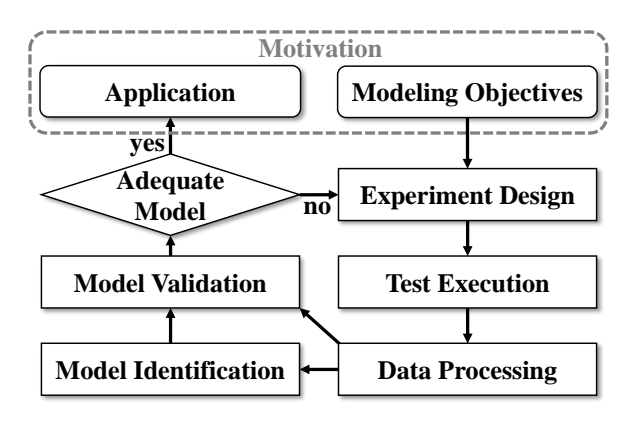


Figure 1: General flight-test system identification process.

Motivation

The system identification effort described in this paper had multiple objectives. First, the stability and control derivatives extracted from flight-test system identification were desired to compare to and validate FLIGHTLAB® predictions. Second, flight-derived modeling results were requested to update and improve the aerodynamic model driving a flight dynamics simulation used for flight control law design. Finally, the flight data and model comparisons were desired to experimentally evaluate and advance the proposed eVTOL aircraft flight-test system identification approach.

Experiment Design

Specific maneuvers are used for aircraft system identification to excite the natural dynamic motion of an aircraft and facilitate collection of informative flight data for model identification. Flight maneuvers employing orthogonal phaseoptimized multisine inputs (Refs. 10, 54-56) are used for this work. A multisine input is defined as a sum of multiple sinusoidal functions with different amplitudes, frequencies, and phase angles, where the frequencies are chosen in a specific frequency band to excite the system dynamics of interest. To make all inputs orthogonal in both the time domain and frequency domain, the multisine signal for the jth control effector is assigned sinusoids with a unique subset K_i of discrete harmonic frequency indices selected from the complete set of K available frequency indices. The available frequencies are $f_k = k/T$, k = 1, 2, ..., K, where T is the fundamental period. For m total control effectors, the jth input signal $u_i(t)$ is defined as,

$$u_j(t) = \sum_{k \in K_j} A_j \sqrt{P_k} \sin\left(\frac{2\pi kt}{T} + \phi_k\right)$$
 $j = 1, 2, ..., m$ (1)

where A_j is the signal amplitude, P_k is the kth power fraction (with $\sum_{k \in K_j} P_k = 1$), ϕ_k is the kth phase angle defined on the interval $(-\pi, +\pi]$, and t is the elapsed time.

The multisine phase angles are optimized to obtain a minimum relative peak factor, thereby helping to keep the aircraft close to its nominal flight trajectory while also retaining the same high input energy as a signal without optimized phase angles (Ref. 10). Because multiple inputs and all aircraft dynamics of interest are simultaneously excited, the use of multisine inputs allows execution of highly efficient and informative flight testing. A single flight maneuver can be used to develop an aircraft dynamic model around a nominal flight condition including nonlinear aerodynamic phenomena and control interaction effects.

For this study, individual multisine signals were generated for each control surface and propulsor, for a total of 16 different excitation signals. Several harmonic components were assigned to each control surface and propulsor multisine signal, where the overall frequency range was set to between 0.05 Hz and 1.85 Hz in accordance with frequencies where the rigid-body dynamics of interest were expected to manifest. For the propulsors, the multisine injections were applied to the squared rotational speed commands $(\Omega_1^2, \Omega_2^2, ..., \Omega_8^2)$, which are the propulsion commands output from the flight control laws, so that the commands are linearly proportional to the

proprotor thrust production. The square root of each squared rotational speed command was taken before sending the output rotational speed command signals to the ESCs. For the control surfaces, the multisine signals were injected directly into the output deflection commands $(\delta_1, \delta_2, ..., \delta_8)$ sent to the actuators.

The input spectra for the final multisine design is shown in Figure 2. The fundamental period of the design is T = 160 seconds and there are 288 total harmonic components, with 18 frequencies assigned to each control effector in an alternating manner. Figure 3 shows the first 10 seconds of the input excitation signals with $A_j = 1$ for the jth control effector; however, a nominal 60-second multisine maneuver length was executed in flight testing.

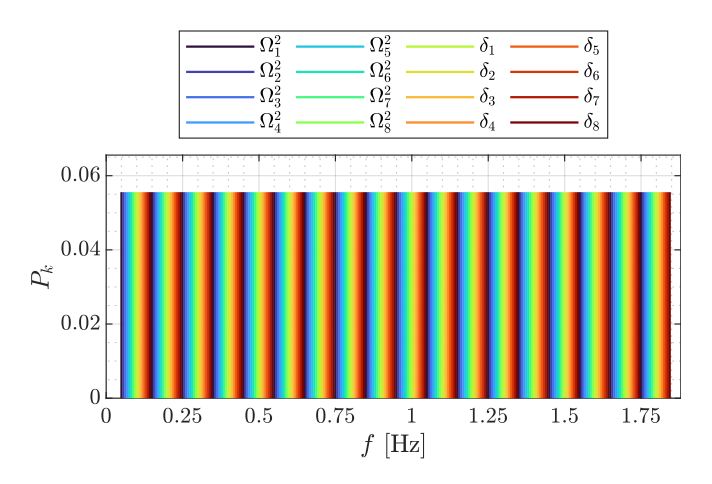


Figure 2: Multisine input spectra for each control effector.

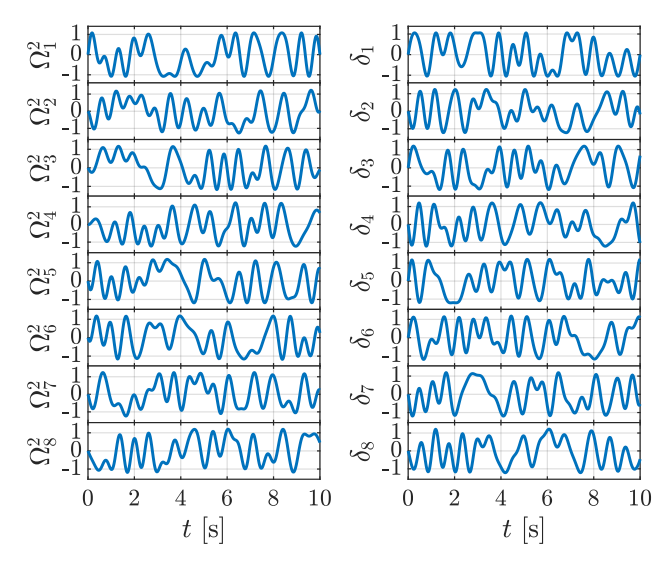


Figure 3: Normalized control effector multisine inputs.

Electric VTOL aircraft are generally unstable for a substantial portion of their operational envelope; therefore, a feedback control system must remain active during system identification flight testing. Although necessary for flight safety, control systems degrade data collected for system identifica-

tion by suppressing natural aircraft motions, distorting designed input waveforms, and introducing correlation among modeling variables. Summing each input excitation signal with the respective control effector command from the control system just before sending the signal to the actuators/ESCs, as shown in Figure 4, is a strategy used to mitigate the adverse effects of the flight controller on system identification results (Ref. 10). Although the control effector commands differ from the optimally designed inputs, injecting multisine signals downstream of the flight control laws generally results in sufficiently low correlation among modeling variables for accurate model identification.

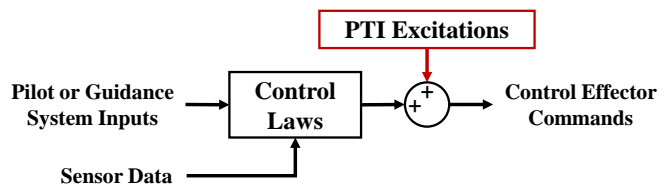


Figure 4: PTI injections relative to the control laws.

For the AIBOT 500 aircraft, the analytical multisine equation and the parameters that specify its attributes (frequencies, power fractions, and optimized phase angles for each signal) were programmed in the flight controller to inject PTIs, as shown in Figure 4. Two adjustable gains were added to scale the motor and control effector PTI commands to sufficient amplitudes to obtain a good signal-to-noise ratio while avoiding significant deviation from the trimmed flight condition or excessively perturbing the aircraft to an unsafe state. The PTI inputs were able to be enabled and disabled in flight by the flight-test personnel to command system identification maneuvers.

Flight Testing

System identification flight testing is conducted on days with low wind and low atmospheric turbulence to best comply with modeling assumptions and reduce uncertainty in the modeling results. A system identification test maneuver is executed by the pilot bringing the aircraft to the desired trimmed flight condition and then enabling the PTI excitations. The pilot retains the ability to make inputs during the maneuver if the aircraft starts to significantly deviate from the original trimmed flight condition; however, the pilot is requested to avoid actively counteracting the PTIs and to make short pulse-like inputs to make corrections. Multisine inputs are symmetric about the trim settings so the necessary corrections are usually minimal. After 60 seconds have elapsed from the start of the maneuver, the PTIs are disabled and the aircraft returns to steady, trimmed flight in its nominal piloted state.

Data Processing

Post-flight data processing is an important step to condition the measured flight data for model identification. For this work, the steps included corrections for time delays, data compatibility corrections, measurement position transformations, and data smoothing. The sensor measurements and state estimates are assessed using kinematic consistency analysis independent of model identification. Corrections only needed to be made for acceleration and angular rate biases, as well as transferring signals from the instrumentation location to the aircraft center of gravity. The sensor measurements and state estimates are all smoothed using a low-pass Butterworth filter applied both forward and backward in time to eliminate phase shift (Refs. 57, 58). For the control surface commands and proprotor rotational speed measurements, time delays relative to the measured aircraft states are removed by systematically varying the time delay in the signals used for modeling and taking the delay that minimizes the mean squared error between the measured and modeled response as the time shift correction. Although control surface position measurements were not available, the control surface command delay correction serves as an adequate model to convert to the position signals required for system identification.

Model Identification

The model identification procedures involve developing an adequate model structure for each response variable and estimating model parameters. The modeling approach focuses on developing polynomial response surface equation (RSE) representations of the response variables as a function of vehicle state and control variables.

Following the approach and justification presented in Ref. 45, individual aero-propulsive models are planned to be identified at several reference flight conditions throughout the flight envelope. The modeled responses are the dimensional body-axis aero-propulsive forces X,Y,Z in lbf and moments L,M,N in ft·lbf. Although the dimensional forces and moments are defined as the responses to be modeled, these quantities cannot be measured directly in flight and must be inferred from other measurements. The dimensional applied forces are calculated as the vehicle mass multiplied by the body-axis translational accelerometer measurements corrected to the aircraft center of gravity:

$$X = ma_x, \quad Y = ma_y, \quad Z = ma_z \tag{2}$$

The applied moments are calculated using the rotational dynamic equations:

$$L = I_x \dot{p} - I_{xz} \dot{r} + (I_z - I_y) qr - I_{xz} pq$$
 (3)

$$M = I_{v}\dot{q} + (I_{x} - I_{z})pr + I_{xz}(p^{2} - r^{2})$$
(4)

$$N = I_z \dot{r} - I_{xz} \dot{p} + (I_v - I_x) pq + I_{xz} qr$$
 (5)

The propulsor transient torque and gyroscopic effects were found to be small relative to the applied aero-propulsive moments and are thus neglected. The body-axis angular accelerations \dot{p} , \dot{q} , \dot{r} within Eqs. (3)-(5) are calculated using smoothed numerical differentiation of the body-axis angular rates (Refs. 10,59).

The explanatory variables are defined as the body-axis translational velocity components u, v, w in ft/s, body-axis angular velocity components p, q, r in rad/s, control surface deflection angles $\delta_1, \delta_2, ..., \delta_8$ in rad, and squared proprotor rotational speeds $\Omega_1^2, \Omega_2^2, ..., \Omega_8^2$ in rad²/s². Each explanatory variable is centered on a reference value to align with the formulation of a multivariate Taylor series expansion.

Similar to the explanation given with the experiment design, the proprotor rotational speed explanatory variables are squared because the proprotor thrust production at a given flight condition is quadratically related to the proprotor rotational speed. In other words, proprotor thrust follows

$$T = \rho A (\Omega R)^2 C_T \tag{6}$$

where ρ is the air density, R is the proprotor radius, A is the proprotor disk area, and C_T is the thrust coefficient (Ref. 60). Therefore, the variations in the squared proprotor rotational speed explanatory variables correspond to linear changes in thrust force production, which improves the agreement with fundamental proprotor aerodynamics and accordingly increases the parameter estimate range of validity.

For this paper, the model structure is composed of linear RSEs used with the nonlinear aircraft equations of motion, which was found to be adequate for local models describing small perturbations around a reference flight condition. The longitudinal responses (X, Z, M) and lateral-directional responses (Y, L, N) include the longitudinal states (u, w, q) and the lateral-directional states (v, p, r), respectively, as regressors. The control variable regressors included in each response are determined using stepwise regression (Refs. 10,61). The final model parameters are then estimated using the equation-error method formulated in the frequency domain (Refs. 10,62).

The control effectors mirrored over the x–z plane presumably have equal effectiveness, but are rarely estimated to be identical due to small physical geometric differences, vehicle asymmetries, and modeling error; however, it is useful in simulation and controls applications for mirrored control effectors to have equal effectiveness and this was a desired model attribute for this work. Therefore, the models are symmetrized by forcing mirrored control effectors to have parameter estimates with equal magnitude in the identification algorithm. This is implemented by adding or subtracting the centered mirroring control effector signals (depending on whether the isolated parameter estimates have the same or opposite signs, respectively) to form a combined regressor used to estimate the symmetrized control effectiveness. As discussed in Ref. 56, a linear combination of orthogonal multisine input signals remains orthogonal to the other orthogonal multisine inputs (or a linear combination of the other inputs), making this model symmetrization approach feasible. For similar reasons, the lateraldirectional response bias parameters were included for estimation, but discarded afterwards to produce a model where the aerodynamics are symmetric about the x-z plane.

Model Validation

After estimating model parameters, validation steps are performed to evaluate if the identified model will be satisfactory for its intended purpose. This includes assessing the ability of the model to predict aircraft motion and inspecting the identified model parameters. Typically, validation flight data withheld from model identification are used to assess model prediction accuracy, where the model should provide a close match to the validation flight data with a similar level of accuracy as the data used for model identification. Individual parameter estimates are also inspected to ensure that they agree with physical intuition and have reasonable uncertainty values. For this paper, validation was performed by assessing the model parameters and comparing the parameters to computationally-derived estimates due to the limited flight data available at the time of publication. Additional model prediction analysis using dedicated validation flight data is planned to be conducted in the future.

FLIGHT-TEST RISK REDUCTION

Although multisine PTI excitations have been successfully and safely applied in numerous aircraft modeling applications (Ref. 16), their use in eVTOL aircraft is newer and best practices for eVTOL applications are still being developed. Therefore, multiple risk reduction steps were taken to ensure safety of flight. First, multisine inputs were applied on a thrust stand with and without the flight-test control system in the loop. The data were used to produce a simple proprotor speed to thrust model from the measured data and assess the physical impact from the multisine inputs, such as extra heating, which were not deemed to present a concern. Then, the multisine inputs were injected into the flight control commands in a flight simulation of the vehicle to determine the expected magnitude of vehicle perturbations relative to the multisine input gains. Both of these initial steps helped to provide an estimate of the necessary multisine input amplitudes that would be required in flight testing. As a final step before performing system identification flight testing, the multisine inputs were injected into the control algorithm and the actual vehicle control effectors in full-vehicle hardware-in-the-loop testing with the vehicle secured to the ground.

After completing these simulation and ground-test based risk-reduction efforts, flight testing was deemed to be permissible with the multisine inputs active. At the start of system identification flight testing, the multisine gains were set to be low and were gradually increased based on pilot and flight-test team assessments. This testing proceeded as expected and ultimately yielded flight data of sufficient quality for initial model identification.

PRELIMINARY HOVER RESULTS

At the time of submission of this paper, initial hover system identification flight testing has been conducted for the AIBOT 500 eVTOL aircraft and the flight data have been analyzed to produce a preliminary hover model. The flight data

from a 60-second hover multisine maneuver are given in Figure 5 and are used for the proceeding analysis. Note that the y-axis scales are removed throughout the presented results to protect proprietary vehicle information.

Following the modeling approach described in the previous section, the parameters in each aero-propulsive force and moment equation were identified using the hover flight data in post-flight analysis. The model structure for each aero-propulsive force and moment was determined to be:

$$X = X_{u}u + X_{w}w + X_{q}q + X_{\delta_{14}}(\delta_{1} + \delta_{4}) + X_{\delta_{23}}(\delta_{2} + \delta_{3}) + X_{\delta_{55}}(\delta_{5} + \delta_{8}) + X_{\delta_{67}}(\delta_{6} + \delta_{7}) + X_{o}$$
(7)

$$\begin{split} Y &= Y_{\nu} \nu + Y_{p} \, p + Y_{r} r + Y_{\Omega_{14}^{2}} (\Omega_{1}^{2} - \Omega_{4}^{2}) + Y_{\Omega_{23}^{2}} (\Omega_{2}^{2} - \Omega_{3}^{2}) \\ &+ Y_{\Omega_{58}^{2}} (\Omega_{5}^{2} - \Omega_{8}^{2}) + Y_{\Omega_{67}^{2}} (\Omega_{6}^{2} - \Omega_{7}^{2}) + Y_{o} \end{split} \tag{8}$$

$$Z = Z_{u}u + Z_{w}w + Z_{q}q + Z_{\Omega_{14}^{2}}(\Omega_{1}^{2} + \Omega_{4}^{2}) + Z_{\Omega_{23}^{2}}(\Omega_{2}^{2} + \Omega_{3}^{2})$$

$$+ Z_{\Omega_{sq}^{2}}(\Omega_{5}^{2} + \Omega_{8}^{2}) + Z_{\Omega_{s7}^{2}}(\Omega_{6}^{2} + \Omega_{7}^{2}) + Z_{o}$$

$$(9)$$

$$\begin{split} L &= L_{v}v + L_{p}p + L_{r}r + L_{\Omega_{14}^{2}}(\Omega_{1}^{2} - \Omega_{4}^{2}) + L_{\Omega_{23}^{2}}(\Omega_{2}^{2} - \Omega_{3}^{2}) \\ &+ L_{\Omega_{58}^{2}}(\Omega_{5}^{2} - \Omega_{8}^{2}) + L_{\Omega_{67}^{2}}(\Omega_{6}^{2} - \Omega_{7}^{2}) + L_{o} \end{split} \tag{10}$$

$$\begin{split} M &= M_u u + M_w w + M_q q + M_{\Omega_{14}^2} (\Omega_1^2 + \Omega_4^2) + M_{\Omega_{23}^2} (\Omega_2^2 + \Omega_3^2) \\ &+ M_{\Omega_{58}^2} (\Omega_5^2 + \Omega_8^2) + M_{\Omega_{67}^2} (\Omega_6^2 + \Omega_7^2) + M_o \end{split} \tag{11}$$

$$N = N_{\nu}\nu + N_{p}p + N_{r}r + N_{\delta_{14}}(\delta_{1} - \delta_{4}) + N_{\delta_{23}}(\delta_{2} - \delta_{3}) + N_{\delta_{59}}(\delta_{5} - \delta_{8}) + N_{\delta_{67}}(\delta_{6} - \delta_{7}) + N_{O}$$
(12)

There is a single parameter estimate for mirroring control effectors (e.g., the parameter $N_{\delta_{14}}$ characterizes the yawing moment control effectiveness of both the δ_1 and δ_4 explanatory variables) following the model symmetrization step explained previously.

Complex least-squares regression (Refs. 10, 62), a frequencydomain equation-error method, was used to determine the final estimates of the model parameters. The hover frequencydomain model fits to the aero-propulsive forces and moments for the multisine maneuver shown in Figure 5 are given in Figure 6. Each subplot also provides the frequency-domain coefficient of determination, R^2 , which characterizes the amount of the response variable variation described by the model. Figure 7 displays the corresponding time-domain model fits compared to the aero-propulsive force and moment data for the same multisine maneuver and using the same model parameters identified from the frequency-domain model identification approach. A good model fit and a high R^2 value is observed for L and M. An adequate model fit, with room for improvement, is observed for X, Z, and N. A lower quality model fit is obtained for Y because there is no direct side force control excitation in hover.

As a result of the injection of orthogonal phase-optimized multisine inputs on each control effector, the control derivative parameters were accurately identified, with parameter estimate percent errors between 4% to 15% for X, Z, L, M,

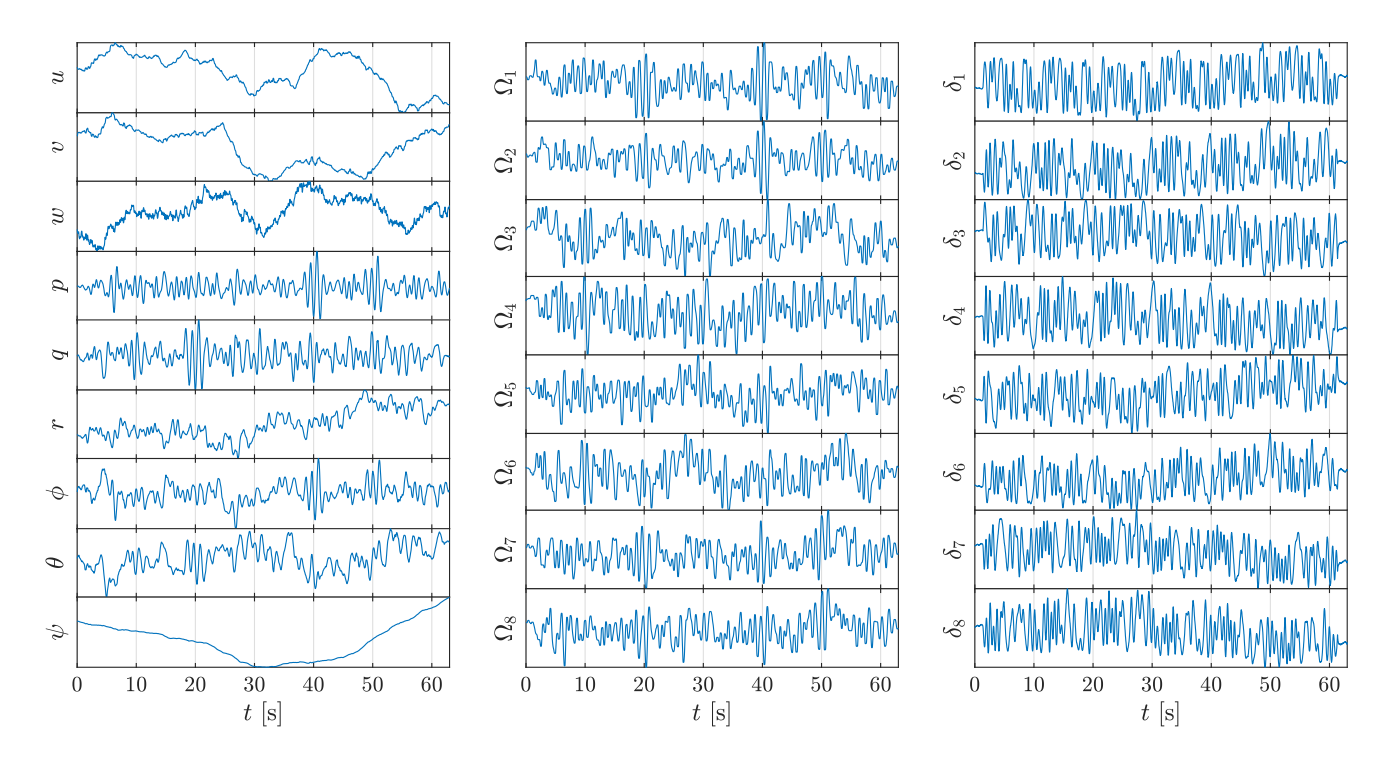


Figure 5: Multiple-input multisine flight maneuver data used for model identification in hover.

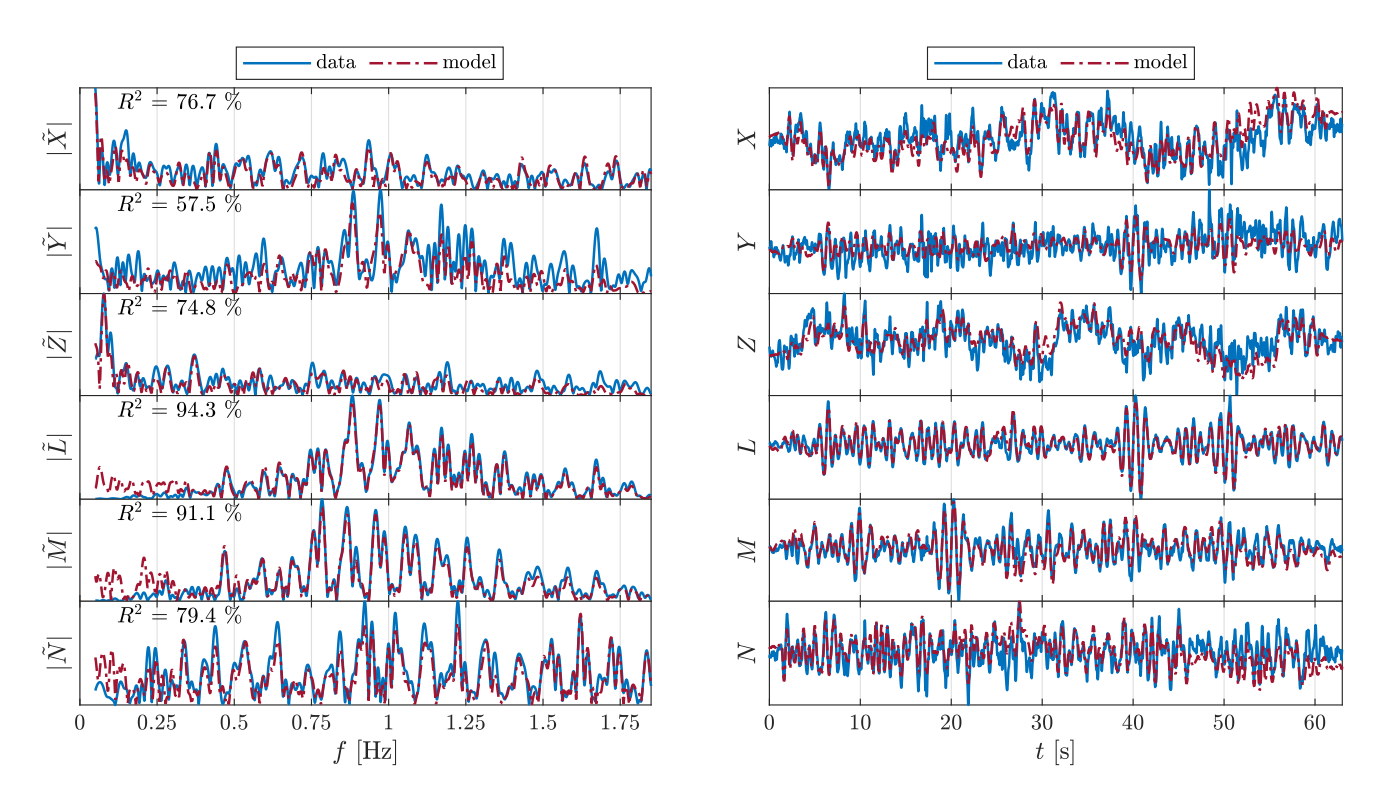


Figure 6: Frequency-domain response data and model fit.

and N; however, the state derivative parameters generally had higher uncertainty estimates. As recently reported in Ref. 46, for some eVTOL vehicle configurations operating at low-speed flight conditions, control effector multisine inputs alone may not provide sufficient state excitation in certain axes for

Figure 7: Time-domain response data and model fit.

accurate identification of the corresponding state derivatives. To resolve this information content deficiency, Refs. 46 and 47 supplemented control effector multisine inputs injected after the flight control laws with additional state command multisine inputs injected before the flight control laws. There-

fore, in subsequent AIBOT 500 flight testing, additional piloted state perturbations were manually commanded alongside the control effector multisine inputs to enable more accurate identification of the state derivatives and improve the overall model fit. Initial hover flight testing applying this improved test execution strategy was conducted in April 2025, right before the submission deadline for this paper. While the multisine inputs were active on each control effector, the pilot sequentially commanded doublet inputs in each axis to provide additional state perturbations during system identification maneuvers. The new results were not able to be included in the paper due to insufficient time before the final submission deadline; however, based on preliminary modeling results using these new flight data, the state derivative identification accuracy and the model fit in certain responses substantially improved with this modified low-speed system identification flight-test execution approach. This finding is a key lesson learned from initial AIBOT 500 flight testing and is recommended to be considered for future eVTOL aircraft system identification efforts applying similar techniques.

One of the objectives of the AIBOT 500 flight-test system identification effort was to compare flight-derived control derivatives to control derivative predictions from FLIGHTLAB®. Figure 8 shows the absolute symmetrized control parameter estimates $\hat{\theta}$ from system identification and FLIGHTLAB[®], with $\pm 2\sigma$ bounds (95% confidence intervals) given on the system identification results. The general control derivative trends show reasonable agreement between the computational and flight-derived estimates. Here, it is important to emphasize the utility and efficiency of applying multisine inputs to each control effector. Using the flight data from only a single 60-second multisine maneuver, the hover control effectiveness parameters for a complex eVTOL aircraft with eight proprotors and eight control surfaces were accurately identified with parameter percent errors less than 15% for each dominant response variable. The flight data collection time is also substantially faster compared to computational and wind-tunnel experiments that provide similar information. Furthermore, although the model identified in this paper was linear, application of multisine inputs to each control effector and the subsequent modeling approach also enables identification of nonlinear model terms, including control interaction effects.

Future system identification flight testing is planned for the AIBOT 500 aircraft in hover, transition, and forward flight. As mentioned above, low-speed system identification testing for the AIBOT 500 vehicle has started implementing additional state command perturbations to supplement the control effector multisine inputs, which improves the state derivative estimates and the overall model fit. In addition to collection of data for model identification, future flight testing will execute additional maneuvers for validation of the identified model. The system identification results are planned to be used to validate FLIGHTLAB® predictions and improve a flight simulation used for flight control algorithm design.

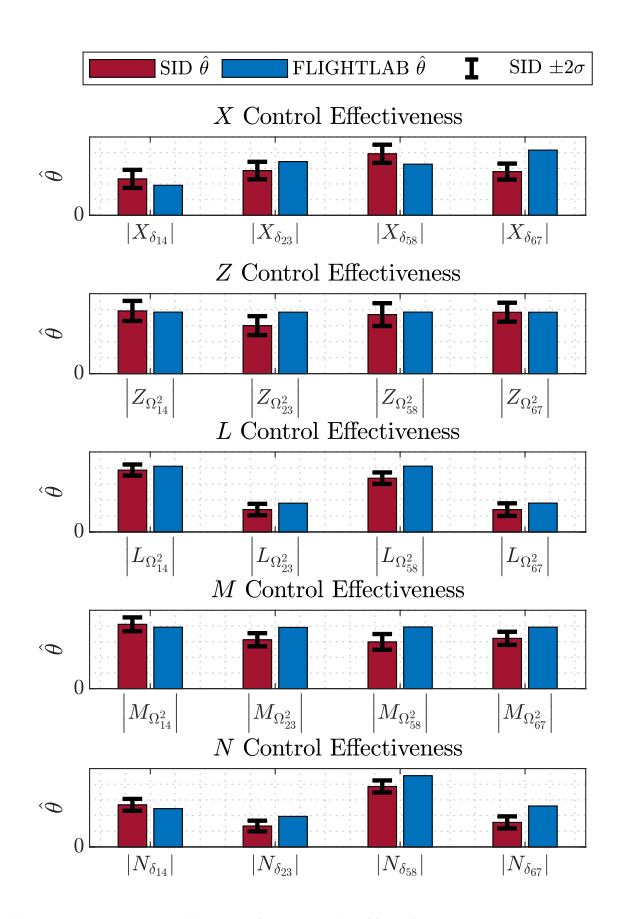


Figure 8: Comparison of control effectiveness parameters derived from system identification (SID) and FLIGHTLAB[®].

CONCLUDING REMARKS

Motivated by computational aerodynamic prediction tool validation and flight simulation improvement, this paper described an ongoing flight-test system identification effort for the AIBOT 500 industry-prototype, vectored-thrust eVTOL aircraft. Although eVTOL aircraft share aerodynamic attributes with both fixed-wing and rotary-wing aircraft, standard system identification approaches must be applied differently for characterizing eVTOL vehicles. AIBOT 500 system identification flight testing was executed by injecting orthogonal phase-optimized multisine inputs into each propulsor and control surface command. Multiple flight-test risk-reduction steps were followed to ensure safe and productive system identification flight testing. Initial hover aero-propulsive modeling results were presented that demonstrated the utility of the system identification approach, while also revealing technique adjustments that will be implemented in future testing to improve the modeling results. The system identification approach enables accurate modeling of complex eVTOL vehicle configurations using a short amount of flight-test time with minimal additional risk posed to the vehicle. Planned future work will apply the system identification approach at different parts of the AIBOT 500 flight envelope to develop a full-envelope aero-propulsive model from flight data. Although the results presented in this paper are preliminary in nature, the practicality, effectiveness, and efficiency of the approach was demonstrated and is recommended for future eV-TOL aircraft system identification efforts.

ACKNOWLEDGMENTS

Support from many AIBOT team members is gratefully acknowledged and appreciated. The first author was funded by the NASA Aeronautics Research Mission Directorate (ARMD) Transformational Tools and Technologies (TTT) project. The collaborative research between NASA Langley Research Center and AIBOT described in this paper was conducted under Nonreimbursable Space Act Agreement SAA1-39241.

REFERENCES

- "eVTOL Aircraft Directory," Electric VTOL NewsTM, https://evtol.news/aircraft, Accessed 31 March 2025.
- Rothhaar, P. M., Murphy, P. C., Bacon, B. J., Gregory, I. M., Grauer, J. A., Busan, R. C., and Croom, M. A., "NASA Langley Distributed Propulsion VTOL Tilt-Wing Aircraft Testing, Modeling, Simulation, Control, and Flight Test Development," 14th AIAA Aviation Technology, Integration, and Operations Conference, June 2014. DOI: 10.2514/6.2014-2999.
- 3. Johnson, W., Silva, C., and Solis, E., "Concept Vehicles for VTOL Air Taxi Operations," AHS Technical Conference on Aeromechanics Design for Transformative Vertical Flight, January 2018.
- Silva, C., Johnson, W., Patterson, M. D., and Antcliff, K. R., "VTOL Urban Air Mobility Concept Vehicles for Technology Development," 2018 Aviation Technology, Integration, and Operations Conference, June 2018. DOI: 10.2514/6.2018-3847.
- Kim, H. D., Perry, A. T., and Ansell, P. J., "A Review of Distributed Electric Propulsion Concepts for Air Vehicle Technology," 2018 AIAA/IEEE Electric Aircraft Technologies Symposium, July 2018. DOI: 10.2514/6.2018-4998.
- 6. Saeed, A. S., Younes, A. B., Cai, C., and Cai, G., "A survey of hybrid Unmanned Aerial Vehicles," *Progress in Aerospace Sciences*, Vol. 98, April 2018, pp. 91–105. DOI: 10.1016/j.paerosci.2018.03.007.
- 7. Johnson, W., and Silva, C., "NASA Concept Vehicles and the Engineering of Advanced Air Mobility Aircraft," *The Aeronautical Journal*, Vol. 126, (1295), January 2022, pp. 59–91. DOI: 10.1017/aer.2021.92.
- North, D. D., Busan, R. C., and Howland, G., "Design and Fabrication of the Langley Aerodrome No. 8 Distributed Electric Propulsion VTOL Testbed," AIAA SciTech 2021 Forum, January 2021. DOI: 10.2514/6.2021-1188.

- Geuther, S. C., Simmons, B. M., and Ackerman, K. A., "Overview of the Subscale RAVEN Flight Controls and Modeling Testbed," Vertical Flight Society's 80th Annual Forum & Technology Display, May 2024.
- Morelli, E. A., and Klein, V., Aircraft System Identification: Theory and Practice, Sunflyte Enterprises, Williamsburg, VA, second edition, 2016.
- Jategaonkar, R. V., Flight Vehicle System Identification: A Time-Domain Methodology, American Institute of Aeronautics and Astronautics, Reston, VA, second edition, 2015. DOI: 10.2514/4.102790.
- Tischler, M. B., and Remple, R. K., Aircraft and Rotorcraft System Identification: Engineering Methods With Flight Test Examples, American Institute of Aeronautics and Astronautics, Reston, VA, second edition, 2012. DOI: 10.2514/4.868207.
- Jategaonkar, R., Fischenberg, D., and von Gruenhagen, W., "Aerodynamic Modeling and System Identification from Flight Data-Recent Applications at DLR," *Journal of Aircraft*, Vol. 41, (4), July 2004, pp. 681–691. DOI: 10.2514/1.3165.
- Wang, K. C., and Iliff, K. W., "Retrospective and Recent Examples of Aircraft Parameter Identification at NASA Dryden Flight Research Center," *Journal* of Aircraft, Vol. 41, (4), July 2004, pp. 752–764. DOI: 10.2514/1.332.
- 15. Morelli, E. A., and Klein, V., "Application of System Identification to Aircraft at NASA Langley Research Center," *Journal of Aircraft*, Vol. 42, (1), January 2005, pp. 12–25. DOI: 10.2514/1.3648.
- Morelli, E. A., and Grauer, J. A., "Advances in Aircraft System Identification at NASA Langley Research Center," *Journal of Aircraft*, Vol. 60, (5), September 2023, pp. 1354–1370. DOI: 10.2514/1.C037274.
- Berger, T., Tobias, E. L., Tischler, M. B., and Juhasz, O., "Advances and Modern Applications of Frequency-Domain Aircraft and Rotorcraft System Identification," *Journal of Aircraft*, Vol. 60, (5), September 2023, pp. 1331–1353. DOI: 10.2514/1.C037275.
- Deiler, C., Mönnich, W., Seher-Weiß, S., and Wartmann, J., "Retrospective and Recent Examples of Aircraft and Rotorcraft System Identification at DLR," *Journal of Aircraft*, Vol. 60, (5), September 2023, pp. 1371–1397. DOI: 10.2514/1.C037262.
- Morelli, E. A., "Flight Test Maneuvers for Efficient Aerodynamic Modeling," *Journal of Aircraft*, Vol. 49, (6), November 2012, pp. 1857–1867. DOI: 10.2514/1.C031699.
- 20. Grauer, J., and Boucher, M., "Identification of Aeroelastic Models for the X-56A Longitudinal Dynamics Using

- Multisine Inputs and Output Error in the Frequency Domain," *Aerospace*, Vol. 6, (2), February 2019, pp. 24. DOI: 10.3390/aerospace6020024.
- Grauer, J. A., and Boucher, M. J., "Aircraft System Identification from Multisine Inputs and Frequency Responses," *Journal of Guidance, Control, and Dynamics*, Vol. 43, (12), December 2020, pp. 2391–2398. DOI: 10.2514/1.G005131.
- Grauer, J. A., and Boucher, M. J., "Real-Time Estimation of Bare-Airframe Frequency Responses from Closed-Loop Data and Multisine Inputs," *Journal of Guidance, Control, and Dynamics*, Vol. 43, (2), February 2020, pp. 288–298. DOI: 10.2514/1.G004574.
- Grauer, J. A., and Boucher, M., "System Identification of Flexible Aircraft: Lessons Learned from the X-56A Phase 1 Flight Tests," AIAA SciTech 2020 Forum, January 2020. DOI: 10.2514/6.2020-1017.
- 24. Perry, A. T., Bretl, T., and Ansell, P. J., "System Identification of a Subscale Distributed Electric Propulsion Aircraft," *Journal of Aircraft*, Vol. 60, (3), May 2023, pp. 702–715. DOI: 10.2514/1.C036616.
- Gremillion, G., and Humbert, J. S., "System Identification of a Quadrotor Micro Air Vehicle," AIAA Atmospheric Flight Mechanics Conference, August 2010. DOI: 10.2514/6.2010-7644.
- 26. Wei, W., Cohen, K., and Tischler, M. B., "System Identification and Controller Optimization of a Quadrotor UAV," AHS 71st Annual Forum, May 2015.
- Niermeyer, P., Raffler, T., and Holzapfel, F., "Open-Loop Quadrotor Flight Dynamics Identification in Frequency Domain via Closed-Loop Flight Testing," AIAA Guidance, Navigation, and Control Conference, January 2015. DOI: 10.2514/6.2015-1539.
- 28. Tobias, E. L., Sanders, F. C., and Tischler, M. B., "Full-Envelope Stitched Simulation Model of a Quadcopter Using STITCH," AHS International 74th Annual Forum & Technology Display, May 2018.
- 29. Sun, S., de Visser, C. C., and Chu, Q., "Quadrotor Gray-Box Model Identification from High-Speed Flight Data," *Journal of Aircraft*, Vol. 56, (2), March 2019, pp. 645–661. DOI: 10.2514/1.C035135.
- Gong, A., Sanders, F. C., Hess, R. A., and Tischler, M. B., "System Identification and Full Flight-Envelope Model Stitching of a Package-Delivery Octocopter," AIAA SciTech 2019 Forum, January 2019. DOI: 10.2514/6.2019-1076.
- 31. Cho, S. H., Bhandari, S., Sanders, F. C., Cheung, K. K., and Tischler, M. B., "System Identification and Controller Optimization of Coaxial Quadrotor UAV in Hover," AIAA SciTech 2019 Forum, January 2019. DOI: 10.2514/6.2019-1075.

- Kaputa, D. S., and Owens, K. J., "Quadrotor Drone System Identification via Model-Based Design and In-Flight Sine Wave Injections," AIAA SciTech 2020 Forum, January 2020. DOI: 10.2514/6.2020-1238.
- Yuksek, B., Saldiran, E., Cetin, A., Yeniceri, R., and Inalhan, G., "System Identification and Model-Based Flight Control System Design for an Agile Maneuvering Quadrotor Platform," AIAA SciTech 2020 Forum, January 2020. DOI: 10.2514/6.2020-1835.
- Ivler, C. M., Rowe, E. S., Martin, J., Lopez, M. J., and Tischler, M. B., "System Identification Guidance for Multirotor Aircraft: Dynamic Scaling and Test Techniques," *Journal of the American Helicopter Society*, 2021. DOI: 10.4050/JAHS.66.022006.
- Leshikar, C., Eves, K., Ninan, N., and Valasek, J., "Asymmetric Quadrotor Modeling and State-Space System Identification," 2021 International Conference on Unmanned Aircraft Systems (ICUAS), June 2021. DOI: 10.1109/ICUAS51884.2021.9476871.
- Niemiec, R., Ivler, C., Gandhi, F., and Sanders, F., "Multirotor Electric Aerial Vehicle Model Identification with Flight Data with Corrections to Physics-Based Models," CEAS Aeronautical Journal, Vol. 13, (3), July 2022, pp. 575–596. DOI: 10.1007/s13272-022-00583-5.
- Niemiec, R., Gandhi, F., Lopez, M. J. S., and Tischler, M. B., "System Identification and Handling Qualities Predictions of an eVTOL Urban Air Mobility Aircraft Using Modern Flight Control Methods," Vertical Flight Society's 76th Annual Forum & Technology Display, October 2020.
- 38. Alabsi, M. I., and Fields, T. D., "Real-Time Closed-Loop System Identification of a Quadcopter," *Journal of Aircraft*, Vol. 56, (1), January 2019, pp. 324–335. DOI: 10.2514/1.C034219.
- Cunningham, M. A., and Hubbard, J. E., "Open-Loop Linear Model Identification of a Multirotor Vehicle with Active Feedback Control," *Journal of Aircraft*, Vol. 57, (6), November 2020, pp. 1044–1061. DOI: 10.2514/1.C035834.
- Figueira, J. C., Bazzocchi, S., Warwick, S., and Suleman, A., "Nonlinear Aero-Propulsive Modeling for Fixed-Wing eVTOL UAV from Flight Test Data," *Journal of Aircraft*, November 2024, pp. 1–13. DOI: 10.2514/1.C037964.
- Kunwar, B., and Chakraborty, I., "Developing Flight Simulation Model for a Lift-Plus-Cruise Subscale Vehicle: Mass Properties, Propulsion, and System Identification," AIAA SciTech 2025 Forum, January 2025. DOI: 10.2514/6.2025-0739.

- Simmons, B. M., and Murphy, P. C., "Aero-Propulsive Modeling for Tilt-Wing, Distributed Propulsion Aircraft Using Wind Tunnel Data," *Journal of Aircraft*, Vol. 59, (5), September 2022, pp. 1162–1178. DOI: 10.2514/1.C036351.
- Simmons, B. M., and Busan, R. C., "Statistical Wind-Tunnel Experimentation Advancements for eVTOL Aircraft Aero-Propulsive Model Development," AIAA SciTech 2024 Forum, January 2024. DOI: 10.2514/6.2024-2482.
- Simmons, B. M., Morelli, E. A., Busan, R. C., Hatke, D. B., and O'Neal, A. W., "Aero-Propulsive Modeling for eVTOL Aircraft Using Wind Tunnel Testing with Multisine Inputs," AIAA AVIATION 2022 Forum, June 2022. DOI: 10.2514/6.2022-3603.
- 45. Simmons, B. M., "System Identification Approach for eVTOL Aircraft Demonstrated Using Simulated Flight Data," *Journal of Aircraft*, Vol. 60, (4), July 2023, pp. 1078–1093. DOI: 10.2514/1.C036896.
- Simmons, B. M., Ackerman, K. A., and Asper, G. D., "Aero-Propulsive Damping Characterization for eV-TOL Aircraft Using Free Motion Wind-Tunnel Testing," AIAA SciTech 2025 Forum, January 2025. DOI: 10.2514/6.2025-0006.
- 47. Simmons, B. M., Ackerman, K. A., Asper, G. D., Gray, M. N., Snyder, S. M., Axten, R. M., Geuther, S. C., and Chan, R., "Subscale Tiltrotor eVTOL Aircraft Dynamic Modeling and Flight Control Software Development," Vertical Flight Society's 81st Annual Forum & Technology Display, May 2025, To be published.
- McSwain, R. G., Geuther, S. C., Howland, G., Patterson, M. D., Whiteside, S. K., and North, D. D., "An Experimental Approach to a Rapid Propulsion and Aeronautics Concepts Testbed," NASA TM–2020-220437, January 2020.
- 49. Montgomery, D. C., *Design And Analysis of Experiments*, John Wiley & Sons, Inc., Hoboken, NJ, 8th edition, 2013.
- Myers, R. H., Montgomery, D. C., and Anderson-Cook, C. M., Response Surface Methodology: Process and Product Optimization Using Designed Experiments, John Wiley & Sons, Hoboken, NJ, fourth edition, 2016.
- 51. "AIBOT," https://www.aibot.ai/, Accessed 14 March 2025.
- 52. "FLIGHTLAB," https://www.flightlab.com/flightlab. html, Accessed 15 March 2025.
- 53. "System IDentification Programs for AirCraft (SID-PAC)," *NASA Technology Transfer Program*, https://software.nasa.gov/software/LAR-16100-1, Accessed 15 March 2025.

- 54. Morelli, E. A., "Multiple Input Design for Real-Time Parameter Estimation in the Frequency Domain," 13th IFAC Conference on System Identification, August 2003. DOI: 10.1016/S1474-6670(17)34833-4.
- Morelli, E. A., "Flight-Test Experiment Design for Characterizing Stability and Control of Hypersonic Vehicles," *Journal of Guidance, Control, and Dynamics*, Vol. 32, (3), May 2009, pp. 949–959. DOI: 10.2514/1.37092.
- Morelli, E. A., "Practical Aspects of Multiple-Input Design for Aircraft System Identification Flight Tests," AIAA AVIATION 2021 Forum, August 2021. DOI: 10.2514/6.2021-2795.
- 57. "FILTFILT: Zero-Phase Digital Filtering," https://www.mathworks.com/help/signal/ref/filtfilt.html, Accessed 31 March 2025.
- 58. Gustafsson, F., "Determining the Initial States in Forward-Backward Filtering," *IEEE Transactions on Signal Processing*, Vol. 44, (4), April 1996, pp. 988–992. DOI: 10.1109/78.492552.
- Morelli, E. A., "Practical Aspects of the Equation-Error Method for Aircraft Parameter Estimation," AIAA Atmospheric Flight Mechanics Conference and Exhibit, August 2006. DOI: 10.2514/6.2006-6144.
- 60. Johnson, W., *Rotorcraft Aeromechanics*, Cambridge University Press, 2013.
- 61. Klein, V., Batterson, J. G., and Murphy, P. C., "Determination of Airplane Model Structure from Flight Data by Using Modified Stepwise Regression," NASA TP-1916, October 1981.
- 62. Morelli, E. A., and Grauer, J. A., "Practical Aspects of Frequency-Domain Approaches for Aircraft System Identification," *Journal of Aircraft*, Vol. 57, (2), March 2020, pp. 268–291. DOI: 10.2514/1.C035599.